Ceramics International 49 (2023) 39745–39759

Contents lists available at ScienceDirect

Ceramics International

journal homepage: www.elsevier.com/locate/ceramint

Review article

Fabrication and environmental applications of glass microspheres: A review

Mokhtar Mahmoud [a,b,c], Jozef Kraxner [a], Hamada Elsayed [b], Enrico Bernardo [b], Dušan Galusek [a,d,*]

[a] FunGlass, Alexander Dubček University of Trenčín, Trenčín, Slovakia
[b] Department of Industrial Engineering, University of Padova, Padova, Italy
[c] Department of Glass research, National Research Centre, Egypt
[d] Joint Glass Centre of the IIC SAS, TnUAD and FChFT STU, Trenčín, Slovakia

ARTICLE INFO

Handling Editor: Dr P. Vincenzini

Keywords:
Additive manufacturing
Environmental applications
Flame synthesis
Glass microspheres
Water purification

ABSTRACT

Continuous technological progress is required to improve production efficiency and environmental quality while maintaining economic competitiveness. A non-negligible contribution to some of these goals can be achieved through the production of glass microspheres for a wide range of applications. The fabrication techniques of glass microspheres including flame synthesis, liquid droplet method, dried gel process and electrical arc process are surveyed. The mechanisms of the recent syntheses of porous and hollow glass microspheres are also reviewed. Glass microspheres are a promising substrate for titania coatings which can be used in water purification and self-cleaning systems. Due to their high mechanical strength and low thermal conductivity, they can also be applied in cementitious and insulating products. Glass microspheres can carry hydrogen gas at pressures of up to 150 MPa. In addition, they can enhance the quality of lead-acid batteries by decreasing the critical volume fraction of the electrodes. Future directions are pointed out on the improvement of the fabrication of 3D glass structures by using glass microspheres as fillers in inks, benefiting from their smooth surface, spherical shape, and high packing density.

1. Introduction

Glass microspheres are spherical particles, typically ranging from 1 to 200 μm in diameter, that can be classified as solid, hollow, and porous. Glass microspheres have been employed for more than 100 years. In fact, solid glass microspheres (SGMs) were produced in New York as far back as 1914. One decade later, a considerable amount of glass microspheres with high refractive index was fabricated for coating movie screens. In 1950, a hollow glass microspheres (HGMs) technology was developed [1–3].

SGMs are manufactured by direct softening of glass powders, while HGMs are produced by adding a blowing (bubbling) agent to the glass powder. Porous glass microspheres (PGMs) can be prepared by several methods, such as alkali activation of glass powder before flame synthesis process or phase separation in SGMs followed by chemical etching. The pores are categorized as 'macro-pores' (>50 nm), 'meso-pores' (50–2 nm), and 'micro-pores' (<2 nm) [4,5].

A combination of the technologies yielding HGMs and PGMs can form porous wall hollow glass microspheres (PWHGMs). First, a blowing agent contributes to the formation of a hollow structure; second, chemical etching on phase-separated glass walls yields products with open porosity and a high surface area [1,6].

Glass microspheres (hollow and porous) are multifunctional materials with a vast number of applications. The combination of thermal resistance, low weight [7], controlled porosity and remarkable strength-to-density ratio opens a number of possibilities to apply these materials in the aeronautics, transportation, automotive [8] and construction industries [9]. PGMs with a high specific surface area are suitable for hydrogen storage [10], thermal insulations [11], floating materials [12] and reflective materials (high refraction index for infrared radiation) [13]. HGMs with porous walls are used as capsules for different elements, e.g. palladium [14], or as filters for the purification of gases [15]. The use of vitreous microspheres in environmental applications represents an economical way to enhance the purity and quality of potable water [16]. Apart from other geometrical shapes, microspheres have favorable properties for biomedical applications, i.e. enhanced ion release, dissolution into tissues and formation of new tissues, drug delivery [17], tissue repairment and regeneration [18].

The main objective of this work is to summarize the preparation

* Corresponding author. FunGlass, Alexander Dubček University of Trenčín, Trenčín, Slovakia.
E-mail address: dusan.galusek@tnuni.sk (D. Galusek).

https://doi.org/10.1016/j.ceramint.2023.10.040
Received 27 April 2023; Received in revised form 3 October 2023; Accepted 6 October 2023
Available online 6 October 2023

List of abbreviation:

BET	Brunauer–Emmett–Teller
BSG	Borosilicate Glass
C–S–H	Calcium Silicate Hydrate
CVF	Critical Volume Fraction
DIW	Direct Ink Writing
DLP	Direct Light Processing
DTA	Differential Thermal Analysis
EDS	Energy-Dispersive X-ray Spectroscopy
FDM	Fused Deposition Modelling
HGMs	Hollow Glass Microspheres
MB	Methylene Blue
N-A-S-H	Sodium Aluminosilicate Hydrate
NIR	Near Infrared
PGMs	Porous Glass Microspheres
PWGMs	Porous Wall Glass Microspheres
ROS	Reactive Oxidizing Species
SGMs	Solid Glass Microspheres
SLA	Stereolithography
SLS	Soda Lime Silica
TGA	Thermogravimetric Analysis
XRD	X-ray powder Diffraction

methods and environmental applications of glass microspheres such as water purification, cementitious materials, gas storage, thermal insulators, thermoplastics materials, improvement of roads and additive manufacturing technology.

2. Preparation of glass microspheres

Many different methods are applied for the fabrication of glass microspheres, including flame synthesis process [18], the liquid droplet method, the dried gel process and the electrical arc plasma [19]. Many sectors depend on glass microspheres as a main constituent in their products and production processes, where they are used as fillers for painting materials. They are also used in countless applications such as aerospace and military materials, molded plastic components, and retro–reflective main road marks [7,12,13].

SGMs have a higher density than HGMs and PGMs, which allows their use in high mechanical strength applications. In turn, HGMs and PGMs are ultra-lightweight inorganic non-metallic materials with hollow structures, and they have multipurpose applications as a new, currently produced material [20,21]. Generally, due to their hollow/porous structure, they are characterized by low thermal conductivity, low density, and good heat preservation properties. Therefore, they can be used in various applications such as water purification systems, thermal insulation materials, catalytic materials, aviation and transportation materials, buoyancy-aid materials for deep-sea applications and structural materials in the aeronautical sector [22–25].

This paper delves into the detailed fabrication processes and techniques for producing SGMs, HGMs, and PGMs. We provide insights into the methods employed, their advantages, and the resulting microsphere properties. This paper section is a comprehensive guide to creating these specialized microspheres. A significant contribution of our work is the exploration of 3D printing as a novel technique for shaping glass microspheres. We highlight the challenges, innovations, and potential applications of 3D-printed glass microspheres. This aspect represents our original research contribution to the field.

2.1. Flame synthesis method

The flame spray method, known as flame synthesis, is a relatively fast and inexpensive technique that can be easily scaled up for commercial manufacturing. In general, the base material is placed in a vacuum powder feeder, which is in direct contact with a vertical or horizontal tube; at the end of this tube is a torch of mixed gases, as shown in Fig. 1. Various studies have applied different gases to produce a flame including propane/oxygen, acetylene/oxygen, petrol/oxygen, hydrogen/oxygen and methane/oxygen [26–28]. Once the particles of glass powder pass through the hot zone along the flame axis, they melt. As an effect of surface tension force droplets of molten glass are converted into spheres, which are quenched in liquid nitrogen, on a cold metal plate or in a water-filled tank. The obtained glass microspheres

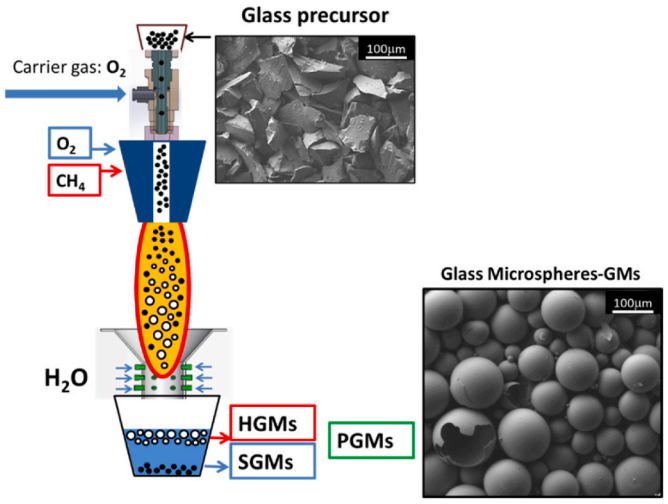

Fig. 1. Schematic diagram of flame synthesis method [19].

then settle down through a sedimentation tank and are subsequently separated by filtration. Typically, the required time for melting the glass is 0.5–10 s, with the time depending on the size of the precursor particles and the gas flow rate [29].

The factors that affect the properties of the obtained glass microspheres can be divided into the properties of the precursors including the particle size, melting temperature, the content of volatile species, chemical and phase composition (which can be obtained by re-melting an already prepared glass, or by having a polycrystalline precursor, or even a mixture of powders that have to react before they can form glass, etc.) and the parameters of the process itself e.g., gas flow rate, combustible gas/oxygen rate and type of the combustible gas. The latter influences both the temperature of the flame, the flame velocity, and the flame emissivity, which all have an impact on the melting process. The initial particle size of the precursor powder is the main factor controlling the formation of dispersed uniform microspheres. The time of the process is also critical as the materials with larger particles require a longer residence time for the glass to spheroidize. Moreover, the flame temperature can influence the dimensions of the obtained spheres significantly and it can be adjusted by using different ratios of the applied gases [30].

Fig. 2 shows various types of glass microspheres and their cross sections after applying the flame synthesis process to glass particles (different glass systems), from the crushing of discarded colorless pharmaceutical containers, composed of borosilicate glass (BSG, a, b), from the soda lime silicate glass waste (SLS, c, d) and PGMs in the bioactive glass SiO_2–CaO–Na_2O–P_2O_5 (e, f) [31]. All microspheres shown in the figure were prepared using a flame synthesis apparatus

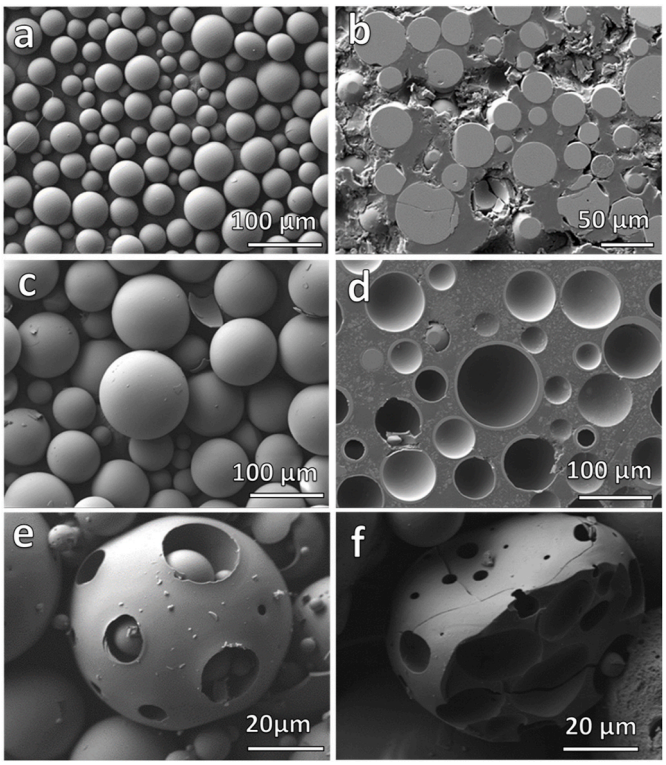

Fig. 2. SEM micrographs of glass microspheres: (a) morphology and (b) cross sections of SGMs prepared from BSG cullet, (c) morphology and (d) cross sections of HGMs prepared from SLS glass cullet, (e) morphology and (f) fracture surface of PGMs prepared from the system: SiO_2–CaO–Na_2O–P_2O_5 [31].

developed and constructed at the FunGlass Center in the Slovak Republic [19].

2.2. Liquid-droplet method

Manufacturing high-quality glass microspheres for special applications requires strict specifications, such as specific diameter and wall thickness tolerance. The Lawrence Livermore National Laboratory developed the liquid droplet method to overcome the problems with a low quality of commercial microspheres [32]. The schematic of this process is shown in Fig. 3. An aqueous solution of glass forming compounds, consisting primarily of sodium silicate, with the addition of small amounts of fluxing agents such as boric acid, lithium hydroxide and potassium hydroxide that decrease the melting temperature is prepared. The liquid is forced through an orifice to form a jet, whose pressure is changed by piezoelectric crystals to produce uniformly spaced droplets. To increase the space between the droplets, some of them are negatively charged by an electrode, deflected, and then removed and collected. Only uncharged droplets pass through the vertical drop furnace. The furnace is divided into four zones and has a vertical span of 5 m. Each part has a characteristic length and temperature that are meticulously prearranged [33].

The velocity of the droplets, i.e., the velocity of the air flow, is controlled by a vacuum vent at the bottom of the furnace. Droplets entering the first zone/encapsulation with a temperature of ~350 °C quickly lose water and a gel membrane forms on the surface. As they pass through the second/drying zone, (T ~ 250 °C), water diffuses out and the gel microspheres inflate. Glass microspheres falling through the third/transition zone (T ~ 950–1050 °C) shrink and are transformed into glass shells, which are refined in the fourth zone (T ~ 1100–1200 °C). Any remaining chemical processes are completed and defects such as bubbles are eliminated. The obtained glass microspheres are collected and cooled down after passing through a fan. As a fundamental drawback, the presented method is time-consuming [34].

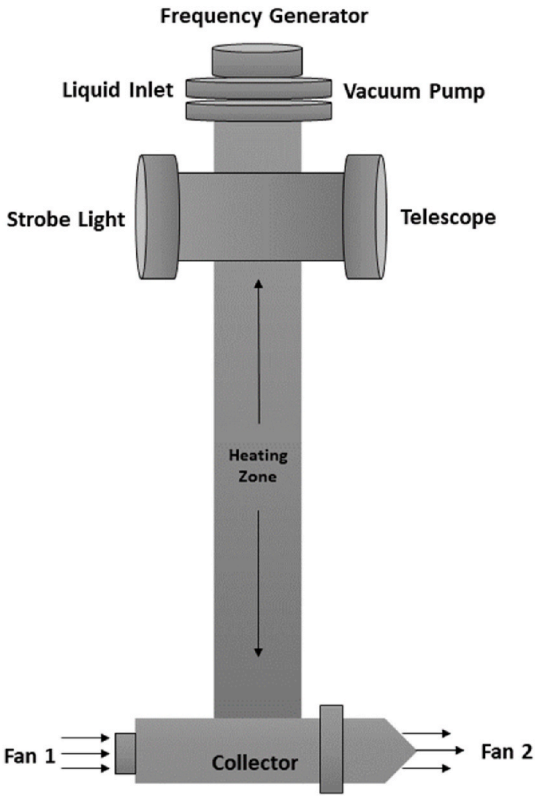

Fig. 3. A schematic diagram of the liquid-droplet method.

2.3. Dried gel process

In this method a gel containing glass forming components and urea is formed and dried for 24 h at 100 °C to remove excess water and methanol [35,36]. The dried gel material is then crushed and dry sieved to have a particle size in the range of 100–150 μm. The product is washed with methanol to remove the waste, which, if present, form bubbles on the surface of the final microspheres. A sized frit is dropped into a three-zone vertical furnace by a vibrating feeder and allowed to fall freely without any updraft. The particles are preheated in the first zone to 900–1100 °C and then blown into spheres in the second zone (1100–1300 °C). Microspheres are stabilized in the last zone (800–1000 °C) before they fall into a water beaker at the bottom of the furnace. All hollow spheres float, while broken spheres sink to the bottom, ensuring the required separation [37,38].

2.4. Electrical arc plasma

The experimental device designed for producing the microspheres in rotating electrical arc plasma is shown in Fig. 4. The arc between electrodes 1 and 2 is supplied by a power supply 3 with a value I of discharge current. Coils 4 and 5 generate a magnetic field such that induction B is perpendicular to the density of discharge current vector j. The interactions between the magnetic field and the current cause the rotation of the electric arc which can be determined by block 6. The feed rate of glass is controlled by the dosing device 7. The cylinder with compressed gas is indicated by block 8. Under the gas pressure, the glass particles, with pre-established flow rate, are carried by the thermally ionized gas. The electrical arc generated in gas medium and rotated by a constant magnetic field is a practical tool for producing glass microspheres [25, 39].

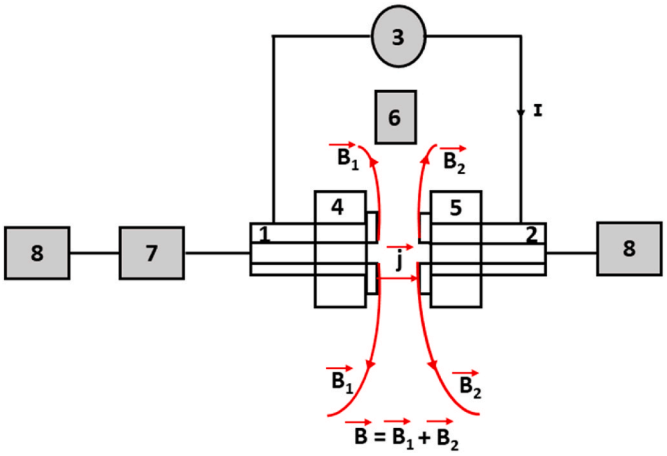

Fig. 4. Schematic diagram of electrical arc plasma (1,2 = electrodes; 3 = current source; 4,5 = coils; 6 = electric arc indicator; 7 = dosing device 8 = compressed gas cylinder) [39].

3. Classification of glass microspheres

The glass microspheres can be classified based on several selection criteria that are briefly summarized below.

(a) Classification by Material Systems
   I. Silica-based glass microspheres: Predominantly composed of silica, these microspheres are chemically inert and are often used in environmental monitoring, sensing, and as additives in paints and coatings [40].
   II. Borosilicate glass microspheres: These glass compositions offer adequate thermal stability, making them suitable for high-temperature applications, such as catalyst supports and thermal insulators [41].
   III. Calcium phosphate glass microspheres: They are a unique class of microspheres with a composition centered around calcium and phosphate ions. These microspheres are of significant interest in various biomedical and materials science applications due to their biocompatibility, bioactivity, and versatile properties [18].
   IV. Composite glass microspheres: Incorporating other materials like polymers or metals into the glass matrix can enhance specific properties, such as electrical conductivity or magnetic responsiveness [42].

(b) Classification by Environmental Fields
   I. Environmental Remediation: Glass microspheres are used to immobilize and encapsulate hazardous waste materials, facilitating safe disposal [43].
   II. Water Treatment: They are employed as filtration media, improving water quality by removing particulate matter and contaminants [44].
   III. Energy Efficiency: HGMs are lightweight fillers in building materials, enhancing insulation and reducing energy consumption [45].

(c) Classification by Main Performance Attributes
   I. Buoyancy: Low density of HGMs makes them ideal for applications requiring buoyancy [12].
   II. Mechanical strength: the inherent strength of glass microspheres allows them to withstand harsh environmental conditions and be applied in road improvement and building materials [46].
   III. Chemical inertness: Glass microspheres resist corrosion and chemical degradation and can be therefore applied in hydrogen storage [47].
   IV. Thermal stability: borosilicate glass microspheres exhibit excellent thermal resistance, making them suitable for high-temperature applications [48].

However, from the point of view of their application, and for the purpose of this review, we consider the classification of glass microspheres based on their morphology, i.e. as solid, hollow, and porous, as the most relevant. Therefore, these types of microspheres are described and discussed in the following sections in more detail.

3.1. Solid glass microspheres (SGMs)

SGMs provide multiple advantages like easy processing, high chemical durability, and thermal stability. SGMs can be prepared by direct melting of a glass base without any additives, using the flame synthesis method. SGMs can also be collected and separated during the preparation of HGMs, as most of SGMs have a density higher than 1.0 g/cm^3 and sink quickly in water [49,50].

In comparison to HGMs, SGMs have a higher density, approximately 2.2 g/cm^3 for borosilicate and 2.5 g/cm^3 for soda–lime glass spheres. They are characterized by a high crushing strength making them suitable for mechanical applications where glass microspheres are subjected to stress during processing or implementation [1].

3.2. Hollow glass microspheres (HGMs)

HGMs, also known as micro–balloons or glass bubbles, have diameters and density changes in the range from 10 to 300 μm and 0.20–0.60 g/cm^3 respectively [51,52]. They are typically made of borosilicate or soda–lime glass batch formulation and are characteristic by such properties as the low density, and high heat and chemical resistance. HGMs can be prepared by applying a blowing agent such as sodium sulfate or urea. The selection of the proper blowing agent is based on its decomposition temperature, which is recommended to be close to the melting temperature of the used glass [51,52].

Wicks et al. prepared HGMs by a flame synthesis method. The particles of glass enter the flame zone, and the flame softens the glass and forms spherical particles. They applied a blowing agent (sodium sulfate) which decomposed at elevated temperatures and formed gas nuclei or bubbles. The bubbles expanded as the glass was heated and formed HGMs as referred to in the following equations [53,54]:

$$Na_2SO_4 \rightarrow^{\Delta} Na_2O + SO_3 \quad \text{Eq (1)}$$

$$SO_3 \rightarrow^{\Delta} SO_2 + \frac{1}{2}O_2 \quad \text{Eq (2)}$$

The amount of sulfur in the glass precursors that may initiate the formation of HGMs during flame synthesis was found to be around 0.3–0.6 wt%. Afterward, the microspheres are quenched in water and collected by flotation. The obtained HGMs prepared in an oxy-acetylene flame have a density in the range of 0.1–0.7 g/cm^3 [53,55].

Kraxner et al. prepared HGMs from automotive glass frit by applying a flame synthesis technique in oxygen/methane flame also using sodium sulfate as the blowing agent. The production of HGMs was influenced mainly by the feed rate of the glass powder into the flame. By decreasing the flow rate from 2.3 to 0.5 g/min the fraction of HGMs increased from 26 to 48 wt% [56].

Dalai et al. prepared HGMs for hydrogen storage by the flame synthesis method, using urea as a blowing agent. They used broken amber glass bottles which were crushed into fine powder using a ball mill, then sieved into 75 μm fraction. The feed flow rate was 100 mg/min, the extent of blowing ranged between 0.3 and 5%. The feed glass powder was sprayed into an oxy-acetylene flame where the viscosity of the glass was reduced, and spherical particles were formed by the action of the surface tension [53].

HGMs can be used as lightweight fillers in composite materials such

as foams and lightweight concrete. They are also applied in submersibles and deep-sea oil drilling devices. Moreover, their capability and ability of low-speed release of pharmaceuticals and radioactive tracers and in hydrogen storage and release represent a significant promise for advanced applications [1,54,57].

3.3. Porous glass microspheres (PGMs)

PGMs are a novel form of glass material consisting of microspheres with a 10 to 100 micron-diameter. The morphological and physical characterization revealed that the porosity of PGMs can achieve up to 76 ± 5% [18,58]. PGMs possess unique properties such as tunable surface area, reactivity, hydrophilicity and hydrophobicity, all of which are beneficial for environmental remediation, separation science, and purification technology. Additionally, PGMs have attracted attention in catalysis, microreactors and biomedical applications [59].

Hossain et al. fabricated PGMs from calcium phosphate glass. They applied a porogen (calcium carbonate) to induce the formation of a porous structure during the flame synthesis using oxy/acetylene flame (Fig. 5a). A glass formulation had to be selected that not only melted but also had a sufficiently low viscosity to allow entrapment of the porogen gas within the molten particles at a temperature that allowed formation of spheres. The morphology is determined by the surface tension of the glass melt when released from a flame. The porogen decomposition rate should ideally be slow enough to trap gases and fast enough to form pores. The obtained PGMS are useful for orthobiologic and biomedical applications [18].

PGMs can also be prepared by applying alkali activation of glass precursors before flame synthesis. In general, any substance that contains a sufficient amount of silica and calcia can be alkali activated. The most common alkaline solutions that can be applied for alkali activation are NaOH, KOH, and sodium silicate hydrates (water glass). The Ca–O, Si–*O*–Si, and Al–*O*–Si bonds are attacked by an alkali solution according to the Glukhovsky model, and the attacked bonds interact to form a coagulated structure [60]. The new phase is responsible for the formation of a condensed structure and crystallization [60]. In a strong alkaline media, the solubility of calcia declines, while the solubility of silica rises [61,62]. In general, for low-calcium precursors, alkaline activation tends to form sodium aluminum silicate hydrate (N-A-S-H) gel with a highly crosslinked structure. In high-calcium precursors, it forms calcium silicate hydrate (C–S–H) gel [63].The hydrated compounds formed by the alkali activation decompose at elevated temperatures, inducing gas evolution, and acting as pore forming agents [31].

Kraxner et al. successfully prepared PGMs based on 45S5 bioactive glass [31]. The glass powder was mixed with an aqueous solution of 1 M NaOH for 1 h under mechanical stirring. The obtained gel was dried overnight in an electric oven at 75 °C. After alkali activation, the XRD analysis confirmed the formation of natrite, C–S–H and sodium hydrogen phosphate hydrate. Alkali activated powder was fed into an oxygen/methane flame at a temperature of around 1600 °C. The hydrated compounds decomposed and released gases such as CO_2 and H_2O which acted as pore forming agents. SEM examination confirmed the formation of a porous structure of the prepared glass microspheres [31].

Mahmoud et al. subjected fiber glass waste to alkali activation in an aqueous solution with different concentrations of sodium/potassium hydroxide, for optimizing the preparation of PGMs. They found out that 9 M KOH was the optimum alkaline solution for inducing porous structure upon the flame synthesis process, using oxygen/methane flame. The activation with 9 M KOH increased the content of K_2O in the glass and shifted the viscosity curve to moderately lower values than 9 M NaOH. The thermogravimetric analysis showed that the use of KOH resulted in a higher weight loss of the activated glass than NaOH, which implies evolution of more gases upon flame synthesis and formation of a more porous structure. The strategy to successfully produce PGMs is to carefully choose the appropriate alkaline activators. A schematic of the preparation of PGMs by the alkali activation method is shown in Fig. 5 b [41].

SGMs and HGMs can be converted into PGMs and PWHGMs by acid leaching with hydrochloric acid after applying heat treatments as shown in the schematic diagram in Fig. 6a. The main role of this process is to produce two different glass phases. For instance, borosilicate system of suitable composition separates into two different phases, one rich in

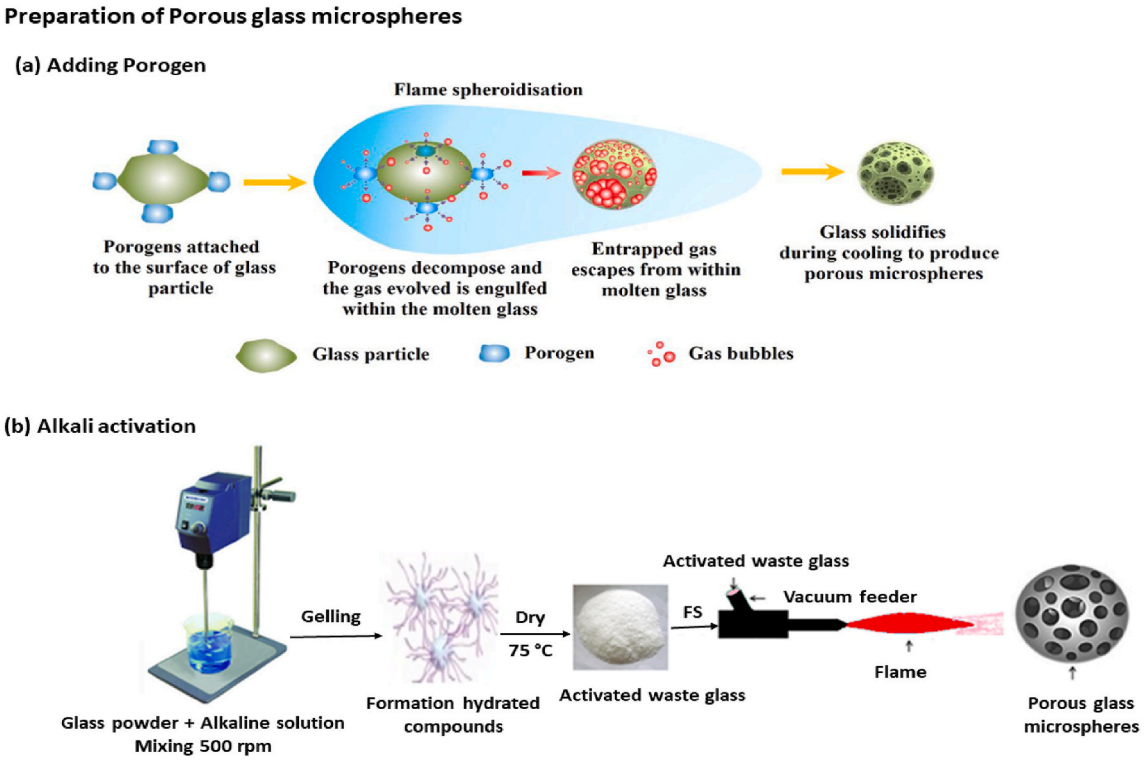

Fig. 5. Schematic mechanism of preparation PGMs by (a) applying porogen and (b) alkali activation during flame synthesis [18,41].

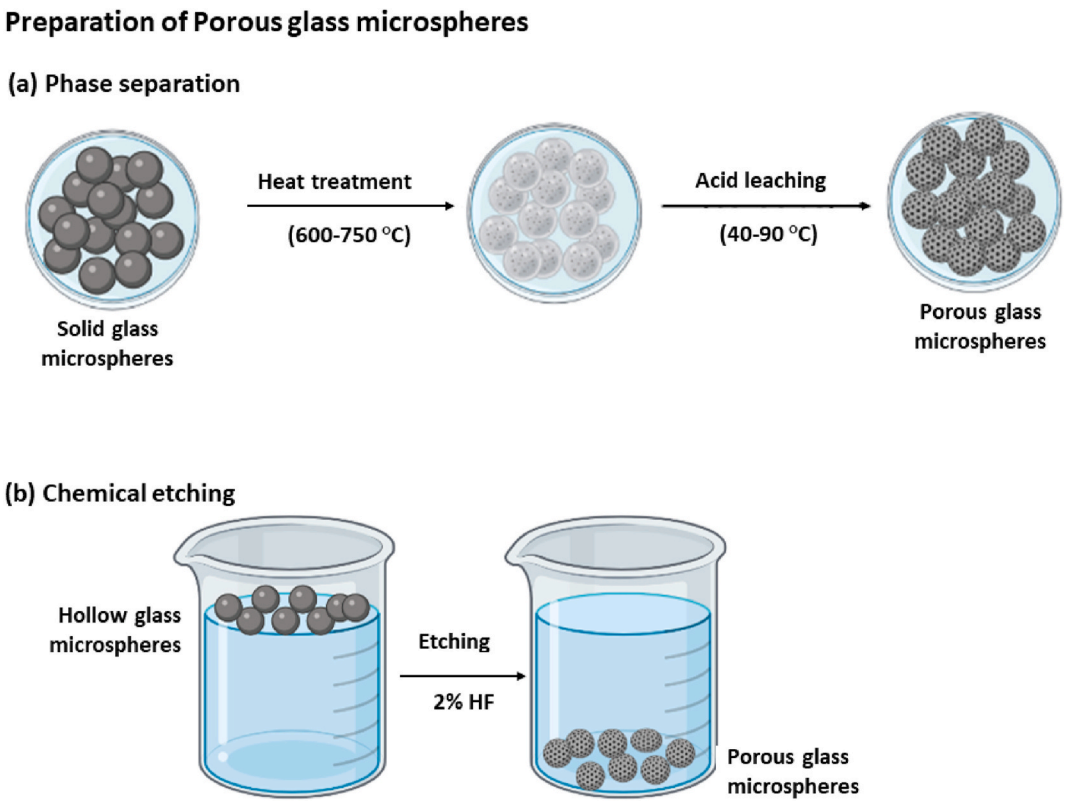

Fig. 6. Schematic mechanism of preparation PGMs by (a) phase separation and (b) chemical etching (Created with BioRender.com).

silica and the other rich in sodium borate [64–66]. The latter always reveals an interconnected wormlike structure, which is then dissolved by acid leaching, forming interconnected pores or channels that extend from the outside of the microsphere shell to the inside [67–69]. Inducing porous structure leads to an increase in the surface area of glass microspheres which enhances the activity of the surface for various kinds of applications.

The obtained material is usually termed as porous glass [70]. Skatulla et al. used a scanning electron microscope to show that phase separation in sodium borate system occurred due to a boron anomaly that is mainly in charge of phase separation and that leachable glasses are not homogeneous [71].

PGMs and PWHGMs can also be produced by chemical etching using hydrofluoric acid that attacks the silica glass shells and forms interconnected pores, as schematically shown in Fig. 6b. This method creates very small pores (nanopores) with diameters in the range of 1–2 nm. Sadabadi et al. produced PWGMs by using 2% diluted HF as a chemical etching reagent using commercial HGMs. Glass samples were ultrasonically cleaned and immersed in the diluted acid under mechanical stirring at 100 rpm. After 5 min, the sample was vacuum filtered, rinsed with 2 % NaOH solution and washed with deionized water. The washed sample was separated into floating HGMs and soaked PWHGMs [72–74].

4. Characterization of glass microspheres

Extensive literature on the topic reports on a number of techniques used in characterization of glass microspheres. Scanning Electron Microscopy (SEM) provides detailed information about microsphere morphology, size, and surface structure. Energy-Dispersive X-ray Spectroscopy (EDS) is used to analyze the elemental composition of the microspheres. X-ray powder Diffraction (XRD) identifies the crystalline phases that can be present in the glass microspheres. Thermogravimetric Analysis (TGA) is employed to determine the thermal stability and decomposition temperature of the porogen. Differential Thermal Analysis (DTA) is used to determine specific temperatures of glass, such as Tg (glass transition temperature), glass softening, and melting temperatures. Brunauer–Emmett–Teller (BET) analysis is used to determine the specific surface area of PGMs. The compressive strength of glass microspheres can be measured using a universal testing machine. Measuring the density helps confirm the quality and classification of prepared glass microspheres. Each type of glass microsphere is usually dedicated to a specific desired application [75–77].

5. Applications of glass microspheres

Glass microspheres, and PGMs with a high porosity in particular, offer unique capabilities for filtration applications. By incorporating absorbents inside the microspheres, they can be also used as a protective agent. This is particularly useful for highly reactive, flammable absorbents or stored materials and offers a great potential in enhancing subsequent safety for handling, storing, or transporting this kind of materials [18,78–81]. In addition to the relative strength of the glass microspheres which can be increased by heat treatment, their mechanical characteristics can be modified. In the following sections, we provide a review of the most important works on glass microspheres and their use in environmental applications.

5.1. Water purification

Water treatment is one of the challenges faced by the whole world due to industrialization, intensive agriculture overusing fertilizers, pesticides and drugs, especially antibiotics, and overpopulation with related overuse of chemicals and pharmaceutical products, including hormonal contraception. Contamination of water resources by organic dyes is of special significance due to their high toxicity and carcinogenicity [82]. Adsorption and photodegradation are ecologically friendly ways of treatment of dye-containing wastewater. Recently it has been reported that these routes were more efficient than coagulation

membrane filtration and biological treatment [83].

Concerning the adsorption process, Samad et al. fabricated PGMs from phosphate-based glasses (using flame synthesis) and studied the effects of heat treatment on their porous structure. They also explored their potential for dye separation from wastewater, using AR88 as an organic reference dye. SEM of heat treated PGMs (510–540 °C) showed a change in the porosity profile; the pore sizes decreased from 55 ± 8 μm to ≤19 nm. The heat-treated PGMs showed a higher dye adsorption capacity (125 mg/g) than the non-heat treated PGMs (83 mg/g). Electrostatic interaction, hydrogen bonding, and Lewis acid–base interaction were determined as the possible mechanisms of adsorption of AR88 onto PGMs [59].

Another recent study investigated the production of PGMs from waste glass (using flame synthesis) and evaluated their applicability for water treatment applications. The obtained PGMs exhibited 69 % porosity with a surface area of 8 m^2/g. The dye removal capability of PGMs from water was investigated for two types of dye (AR88 and MB). The maximum monolayer adsorption capacity of PGMs was 78 mg/g and 20 mg/g for AR88 and MB dye, respectively. The PGMs showed good recovery with almost stable efficiency (86–87 %) over 5 adsorption cycles [44].

This method comes with its own set of challenges that need to be overcome for effective and efficient dye removal. Here, we discuss some of the key challenges associated with using PGMs for dye remediation. PGMs are known for their high surface area and porosity, which make them excellent candidates for adsorption-based dye removal. However, the challenge lies in optimizing their adsorption capacity [44]. The selection of appropriate pore sizes, pore volumes, and surface functionalization is crucial to maximize the uptake of dyes. Different dyes have varying chemical structures and properties, which can influence their affinity for PGMs thus making the microspheres dye-specific agents [59]. Therefore, achieving broad-spectrum adsorption capability is challenging, as the system may be more effective for certain dyes while less efficient for others. Another significant challenge is balancing the performance of PGMs with their cost-effectiveness. Developing affordable materials and processes for dye remediation without compromising efficiency is essential for widespread adoption [59].

Regarding the photodegradation process, the most traditional photocatalysts are TiO_2, ZnO, $BaTiO_3$, $SrTiO_3$ etc. [84]. A TiO_2 photocatalyst with nano-sized particles shows the best performance. However, for practical application TiO_2 needs to be coated on a suitable substrate (e.g. glass microspheres) which may result in the peel off of the coating films from the substrate, leading to a short service life [85]. For inducing photocatalytic activity in bulk glass microspheres, it is necessary to precipitate photocatalytic crystals on their surface [86]. Laser induced crystallization is a successful technique to grow the desired photo catalytically active crystals on the surface of glass microspheres. Such crystallization of TiO_2 on the surface of glass may overcome the problem with the peel-off of the coating films. TiO_2 exists in three stable crystallographic modifications of TiO_2: anatase, rutile and brookite. Anatase exhibits the highest photocatalytic activity. Accordingly, glass-ceramics containing anatase type TiO_2 crystals are required [87].

Schematics of pollutants degradation on a photocatalytically active surface are shown in Fig. 7. Reactive oxidizing species (ROS) react with adsorbed pollutants, such as organic compounds, decomposing them in the process. The products of the photocatalytic reactions are carbon

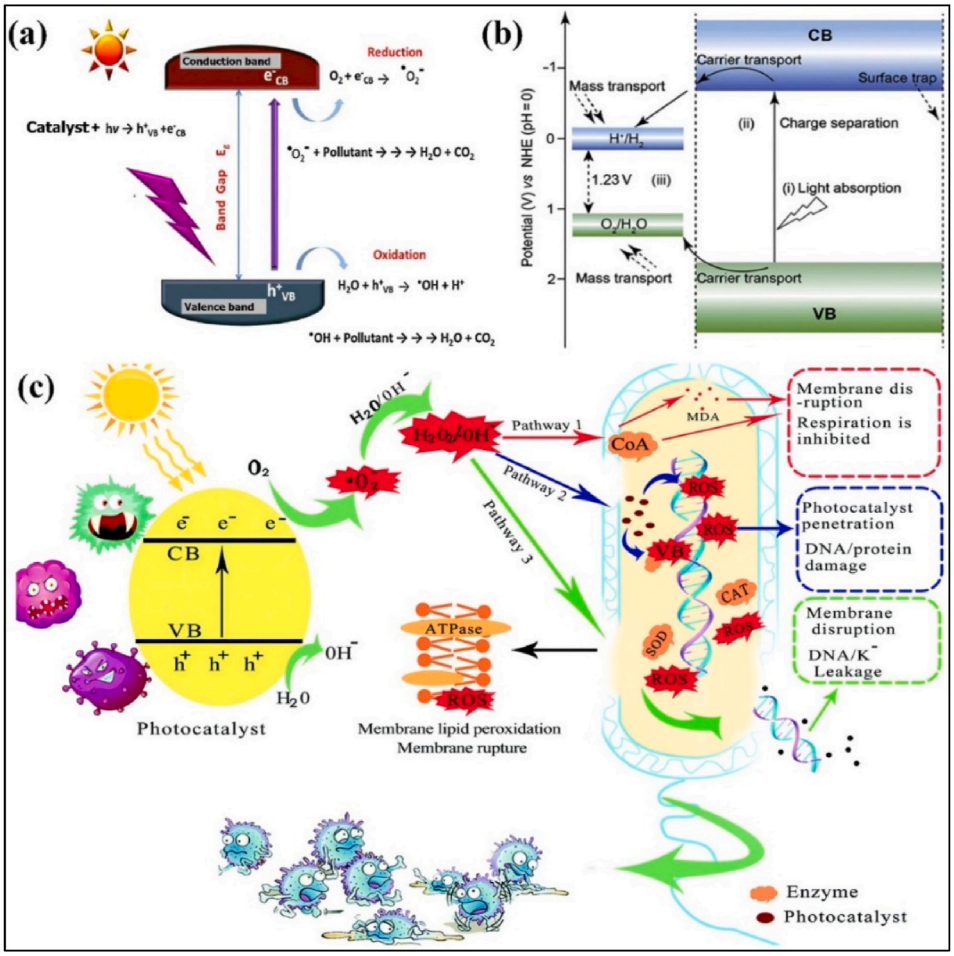

Fig. 7. Schematics of the mechanism behind the photocatalytic degradation of organic pollutants (a), hydrogen evolution (b), bacterial disinfection (c) [84].

dioxide and water. The mechanism of TiO_2– induced photocatalysis of the degradation of organic pollutants is illustrated in Fig. 7a.

Photocatalysis can be also applied for hydrogen production by photocatalytic water splitting. The mechanism includes the surface reaction of photogenerated electrons (e^-) with water, yielding hydrogen (H_2), and holes resulting in the evolution of oxygen (O_2) (Fig. 7b).

ROS generated in an aqueous medium can also enter bacterial cells, stimulating oxidative stress, which initiates peroxidation of the lipid membrane. ROS targets proteins, impairs the activity of various periplasmic enzymes, interact with DNA and damages it. The schematic of the photocatalytic disinfection mechanism is shown in Fig. 7c [84].

Zhang et al. used a sol gel method to coat chromium, sulfur, and titanium dioxide on commercial HGMs for photocatalytic degradation of indigo carmine (a dye used in the textile industry) under visible light. After calcination, the surface of HGMs was covered by a dry gel, and the XRD confirmed the formation of anatase crystals [88]. The absorption wavelength of pure TiO_2 is less than 400 nm, while the absorption spectra of the loaded materials (chromium, sulfur, and titanium dioxide) of HGMs range deeper into the visible light region. As a result of the coating, the specific surface area of the Cr/S/TiO_2-HGMs increased from 132 to 176 $m^2\ g^{-1}$. The photocatalytic activity was estimated by the degradation of the dye induced by visible light. The observed degradation efficiency of indigo carmine was 98.06 % and the time of degradation was 1.5 h. The specimens fired at 80, 300 and 400 °C showed negligible photocatalytic activity while 500 °C was found to be the optimum calcination temperature of anatase crystallization [88].

Yanyan et al. functionalized HGMs as a self-floating adsorbent for wastewater treatment by co-grafting polydopamine onto HGMs made from borosilicate glass for producing an efficient polydopamine shell structure adsorbent [89]. The smooth surface of HGMs was pretreated by 0.5 mol L^{-1} NaOH to form PWHGMs. The specific surface area increased from 2.04 m^2g^{-1} (before etching) to 26.62 m^2g^{-1} (after etching). The adsorption capacity of the functionalized HGMs for alizarin cyanine green F dye was 64 mg/g. The removal efficiency of 0.10 m mol L^{-1} dye solution reached 94.51 %, and the adsorption process reached an equilibrium within 1 h. The adsorbent has exceptional recyclability, and its adsorption quality can be maintained for several cycles [89].

Using the same principle of dye degradation for wastewater treatment, Gunnarsson et al. successfully studied the preparation and characterization of TiO_2-coated HGMs for self-cleaning paints. The photocatalytic activity was assessed by following the degradation of methylene blue (MB, organic dye) as a function of time under UV exposure, by immersing coated HGMs in an MB solution [90]. For the assessment of self-cleaning behavior, alkyd paints comprising both uncoated and coated HGMS were prepared. Several drops of aqueous MB solutions were then applied to the surface of the paint and were allowed to dry out. The panels were then exposed to UV light and photographed after 28 and 52 h of exposure. The dye on the film containing coated HGMs was completely eliminated after 28 h of exposure [90].

5.2. Thermal insulation

HGMs possess low thermal conductivity, so they are considered promising materials for thermal insulation. Bing et al. studied the impact of the structure and physical factors which directly affect the insulation quality, targeting the direct relation between density and thermal conductivity [91].

Generally, the basic mechanism of heat transfer in HGMs is conduction. As observed by Skochdopole, natural convection in porous materials cannot practically occur in the presence of bubbles with a diameter below 4 mm [92]; this is fulfilled for HGMs, whose diameters are usually below 100 μm. The main factors controlling the conduction are density, heat transfer path, and contact points. The thermal conductivity of the system can be decreased by increasing the volume of the gas, by increasing the ratio of the internal and external diameters of the prepared microspheres (method I), or modifying the stacking of microspheres of different diameter, as in method II (Fig. 8) [92].

The density of HGMs can be calculated by equation (3)

$$\rho = [1 - (d/D)^3]\ \rho_0 \quad \text{Eq (3)}$$

where d is the average internal diameter of the microspheres, D is an average external diameter of the microspheres, and ρ_0 is the density of the solid phase. With any d/D change, the density varies significantly; high d/D ratios are generally associated with a significant decrease in thermal conductivity, especially for stacked microspheres [92].

Jie et al. studied TiO_2-coated HGMs to enhance their insulation properties. Coating and growth of TiO_2 colloid on the surface of HGMs required the formation of a multidimensional network that can be formed by crosslinking and condensation of TiO_2 particles [93,94]. The thermal conductivity of the uncoated HGMs was 0.0575 W/(m·K), and their near-infrared (NIR) reflectance was 88.31 %, while the thermal conductivity of coated HGMs increased to 0.0623 W/(m·K), and the NIR reflectance was 96.27 %. Increasing the amount of TiO_2 significantly improved the reflectance and thermal insulation properties of the TiO_2 film/HGMs composites, although the thermal conductivity of the TiO_2 film/HGMs composites increased slightly. The inner surface temperature of the composite coated on the aluminum board was reduced by 22.4 °C which indicates an excellent solar reflective and thermal insulation properties [93].

Most convective heat transfer can be prevented by the cavities in the HGMs. However, the absorption and transfer of infrared and visible wavelengths by radiation can diminish the thermal insulation performance of HGMs [95]. The formation of a core/shell structure by coating near-infrared (NIR) reflective layers on HGMs can efficiently decrease heat transfer from solar radiation. Titania attached to the surface of microspheres can thus create core/shell composite materials with low thermal conductivity.

5.3. Glass microspheres in building materials

More than 10% of global CO_2 emissions are coming from the concrete industry [45]. In recent years, many researchers have been working on the development of sustainable forms of concrete using recycled materials. Aslani and Wang incorporated HGMs into lightweight cementitious composites. The HGMs with three different densities of 0.25, 0.40, and 0.60 g/cm^3 were considered as lightweight fillers, with two different volumetric fractions (40 and 60 %) [45]. Composites can be applied in some critical structures such as floating concrete platforms and long suspension bridges.

The compressive strength of the lightweight cement composite prepared in this work depended mainly on the strength of HGMs used in the mixture. By adding 40 and 60 % of 0.25 g/cm^3 HGMs, the flexural strength increased by 10 % in comparison to the reference sample, although the compressive strength was reduced by 10–30 %. The addition of HGMs with a density of 0.40 g/cm^3 into the lightweight cementitious composite caused a slight reduction of the compressive and flexural strength. HGMs with a density of 0.60 g/cm^3 showed the opposite effect. With the addition of 40 and 60 % of HGMs, the flexural and compressive strength respectively increased by 9.6 and 7 %. The surfaces of low density microspheres remained smooth, without any interaction with the cement, while denser particles reacted with the surrounding matrix [45].

Oreshkin et al. studied lightweight extruded masonry mortars with added HGMs. The incorporation of HGMs helped to produce a material with a higher homogeneity, high strength/density ratio, and excellent thermal resistance [96]. Kumar et al. evaluated lightweight, high-strength polypropylene-based hybrid composites comprising HGMs and fibers. The addition of HGMs caused a decrease in the tensile strength, while the flexural strength increased [97].

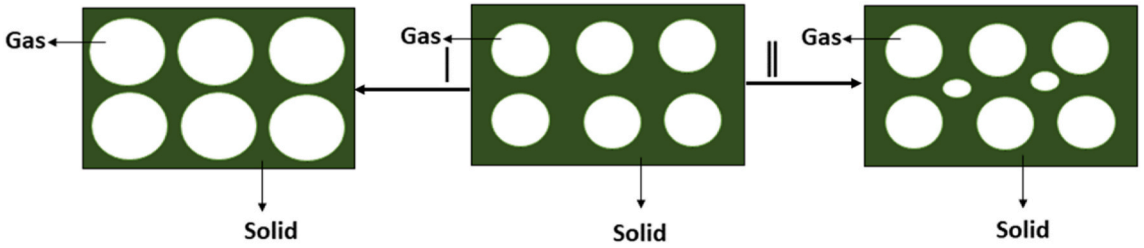

Fig. 8. Method I for expanding the volume of the hollow part of HGM; method II for rising the quantity of HGM.

5.4. Hydrogen storage

The storage of compressed hydrogen gas in HGMs provides great benefits such as high efficiency, safety, lightness, cheapness, and simplicity in storage system design [98,99]. The main factor that allows HGMs to work successfully in this application is their relatively high strength. Due to their small diameters, they have the ability for storing hydrogen in gaseous form at pressures up to 150 MPa. In addition, HGMs are safe and non-explosive, because each individual microsphere stores only a very small volume of hydrogen gas. HGMs are thus a suitable alternative to metal cylinders [100,101].

Hydrogen storage ability of HGMs is influenced by the diffusion of hydrogen through the glass shell at high temperatures and its ability to sustain high pressures of hydrogen gas for a long time. The diffusivity of H_2 in HGMs required for efficient hydrogen loading and unloading is favorable, usually requiring the temperatures used for filling and outgassing above 300 °C [102–104].

There are two different approaches for enhancing the diffusivity of hydrogen gas in HGMs. The first way is to create some micro cracks in the glass shell wall as a diffusion path for gases. The second way is to decrease the ratio of glass modifiers such as alkali oxides in order to expand penetration channels in the glass network for hydrogen gas, as the glass modifiers on the interstitial holes in the silica matrix essentially block the hydrogen diffusion through the glass network. However, the first way is often not feasible, because it significantly affects the strength of HGMs. For the second way, borosilicate glass systems with lower viscosity at the working temperatures is recommended [105].

Xiaobo et al. studied the influence of initial glass composition, blowing agent, furnace atmosphere pressure, refining temperature, the diffusion time, quality and yield of the resulting HGMs. The main objective was studying high diffusivity HGMs for hydrogen storage through volatilizing alkali and boron content in the shell-forming process. They found that 15%–20% is the optimized ratio for alkali oxides for producing a high silica matrix of HGMs with extraordinary performance. The permeability coefficients of the high silica HGMs to hydrogen gas at ambient temperature are between 3 and 4 x10^{-20} (mol m)/(m^2.s.Pa) [106].

Dalai et al. reported that the amount of hydrogen gas stored at HGMs (made from amber glass bottles) at 200 °C was higher than at room temperature. At this temperatures hydrogen diffuses faster across the microsphere wall into a hollow cavity inside. This study confirmed that more pores at the surface of HGMs led to a higher hydrogen uptake. The HGMs prepared with 2 % urea (blowing agent) showed a large number of micro/nano pores and it showed a hydrogen storage capacity of 2.3 wt % at 200 °C and 10 bar pressure [53].

Determining the "best" system of glass microspheres for hydrogen storage depends on various factors, including the specific requirements of the application, the desired hydrogen storage capacity, operating conditions, safety considerations, and cost constraints. Several glass microsphere-based systems have been explored for hydrogen storage, and each has its advantages and limitations [103,107].

Due to their chemical inertness and high surface area, silica-based glass microspheres are a common choice for hydrogen storage. They can be engineered with porous structures to enhance hydrogen adsorption. Silica microspheres have shown promise in achieving moderate hydrogen storage capacities at ambient temperatures and moderate pressures. They are considered safe and have good thermal stability [100].

Composite glass microspheres incorporate other materials, such as metals or metal hydrides, into the glass matrix. These systems aim to combine the high hydrogen storage capacities of metal hydrides with the structural benefits of glass microspheres. The choice of metal hydride and glass composition plays a crucial role in determining the storage capacity and kinetics [108].

Coated Glass Microspheres: Glass microspheres can be coated with materials that enhance hydrogen adsorption. For example, they can be coated with catalysts, metal nanoparticles, or other hydrogen-absorbing materials. The coating enhances hydrogen adsorption and desorption kinetics while maintaining the structural benefits of the glass microspheres [47].

5.5. Lead acid batteries

Glass microspheres with controlled porosity are promising for energy storage applications. They can be utilized as components in advanced batteries and supercapacitors, where their tailored structure can enhance energy density and charge-discharge rates [109]. Lead acid batteries have been used for several decades due to their high capacity and low cost [109]. Berndt calculated the theoretical capacity of lead acid batteries to be as high as 166 Wh kg^{-1}, although in practical work the energy efficiency of these batteries is usually only around 30 Wh kg^{-1}. This lack of efficiency may be attributed to only about 60 % of the theoretical active material of the negative plate and 50 % of the positive plate that can react. The main reason for this lack of performance is that a large amount of unreacted active material takes part in the total weight but supplies no energy for the battery [110]. Actually, this happens also when the active material becomes completely discharged and it is no longer conductive, so parts of the active material become electrically isolated and cannot work anymore, becoming the so-called 'dead weight' [111].

Significant effort has been therefore focused either on the increase of the active part or the decrease of the dead part. Edwards et al. worked on replacing the dead part of the active materials by using PWHGMs of different sizes. PWHGMs were used for increasing electrolyte storage and enhancing specific energy efficiency. Matthew et al. studied the use of PWHGMs as paste additives that enhance the porosity of active materials in positive electrodes. Computer simulations showed that using approximately 20 % by volume of porous materials enhanced specific energy performance to approximately 40W h kg^{-1} [112]. Two different kinds of glass microsphere systems (borosilicate glass, soda lime silica glass) were used. All samples were soaked in a 1% HF for 20 min to obtain a porous wall structure. The addition of PWHGMs decreased the critical volume fraction (CVF) of the electrodes, improving the quality of electrode performance [112].

5.6. Thermoplastics

HGMs significantly contributed to the development of the

thermoplastics industry. The main reason for introducing HGMs to the polymers was to decrease the cost related to the use of a high quantity of resin. The fillers are also expected to enhance the mechanical and physical properties of the polymer. In the past, most fillers such as glass fibers and talc had a higher density than the host resin which resulted in a net product with excessive weight. Recently, this problem was addressed by incorporating low density HGMs [113].

Ding et al. developed a method for fabricating co-continuous HGMs/epoxy resin syntactic foams with low density and excellent compressive properties as an alternative to the traditional stir-casting method. Instead of direct mixing of HGMs with the epoxy resin followed by degassing and applying a vertical pressure, with subsequent casting and curing as in the traditional method shown in Fig. 9, HGMs were poured into a quartz tube under continuous vibration followed by a vertical pressure to make HGMs close-packed. Then the epoxy resin was injected under vacuum. Afterward, the resin overflowed from the outlet of the mold, as outlined in Fig. 10. The latter method eliminates matrix porosity, making experimental density almost the same as theoretical density of the syntactic foam, which provides minimum porosity and decreases the number of defects in the composite. In addition, it solves a common problem of the products prepared by conventional methods, such as presence of pores and air bubbles that need to be degassed [114].

The analysis of the deformation mechanisms at the microscale demonstrated that matrix pores were the main factors reducing the mechanical performance of the composites. The compressive strength and modulus of the composites prepared by this new method were 45.3 % and 37.6 % higher than for those prepared by the conventional method, and the water absorption was 69.9 % lower. The low density, low moisture absorption and high compressive strength of the fabricated composites make them excellent buoyancy materials for deep-sea exploration.

Decreasing the density of thermoplastic parts is a desired goal in various industries including aerospace, electronics and transportation. HGMs are applied for lightweight automotive applications including thermoplastics, foaming materials, sheet and bulk molding composites. Replacing the higher density fillers with HGMs showed great benefits, for instance, decreasing density by up to 13 % and increasing dimensional stability of injection molded automotive parts. Introducing HGMs into high-temperature polymers such as polyetherimide reduced the total weight by 10 % and resulted in a lower cost in comparison to glass fiber reinforced composites [115].

Along with density decrease, the incorporation of HGMs in thermoplastics provides additional advantages including faster cooling rates, higher dimensional stability, increased thermal resistance and decreased thermal conductivity. Cooling of the thermoplastic objects from the melt is a critical point from an economically point of view because long cooling times impair the production output [116]. Higher cooling rates are achieved due to their influence on thermal diffusivity, through the introduction of HGMs into thermoplastics. By increasing the HGMs ratio, the composite density and specific heat capacity decrease, which in turn enhances the thermal diffusivity and cooling rates [117].

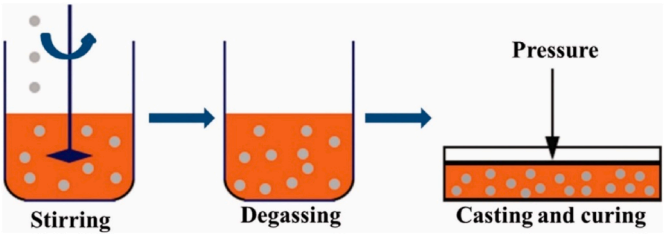

Fig. 9. Schematic of the of the conventional stir-casting method [114].

5.7. Road improvement

The main material used for road construction is asphalt, which is used as a glue or binder mixed with aggregate particles to create asphalt concrete [27,46]. Because of its black color, it possesses a high solar absorption rate. In the summertime, asphalt pavement absorbs a large amount of heat so that the road surface is extended and distorted [118]. Elimination of the negative impact of the high temperature on the road surface is a primary goal of several published works [118]. The techniques of solar reflective coating [119] and thermal resistance pavement [120,121] have been developed several years ago to facilitate the cooling of asphalt pavement. The cooling is facilitated by rising the void percentage in the pavement or adding a material with a lower thermal conductivity into the asphalt mixture to decrease the thermal conductivity of the asphalt.

HGMs combine good mechanical properties, low density and relatively affordable cost of production. Good thermal insulation properties make HGMs widely applicable [122]. Feng et al. studied the incorporation of HGMs into asphalt pavement for lowering the temperature of the road surface [46]. It was found that the increasing ratio of HGMs led to a decrease in the penetration and ductility, while the softening point increased. Moreover, the high temperature shear resistance of asphalt increased [46].

5.8. Additive manufacturing technology

Additive manufacturing (3D printing) technology has been utilized in many production processes as a rapid prototyping tool. The only exception was the production of 3D glass structures, whose processing remains a challenge. The technology of 3D printing has been developed for more than 30 years [123] and nowadays its utilization covers various areas, including the construction of houses [124–126]. In recent years, 3D printing devices have become cheaper and simpler to use, which has led to the rapid development of applications of this technology. As a new rapid fabrication method, 3D printing brings many new possibilities to the field of catalysis. Structural design, control of catalyst distribution, and the fabrication of monolithic reactors are becoming easier [124–126]. However, novel printing materials and optimized catalyst designs are still needed to achieve even better catalytic performances. With the depletion of fossil fuel resources and increasing environmental concerns, 3D printing fabrication provides new solutions for preparing catalysts with new structures in a more economical and energy-efficient way. Overall, the field of 3D printing as a manufacturing technique is a new paradigm in new material design and fabrication that have wide promise in water-related applications. In the last few years, there has already been an advancement in 3D printing. However, some 3D printing materials, processes such as glass part printing, cost and post-processing parameters and even its environmental and health impacts need to be addressed in order to fully realize their unlimited potential [123].

The glass/glass-ceramics additive manufactured 3D structures were mostly prepared by Direct Light Processing (DLP), Stereolithography (SLA) or Direct Ink Writing (DIW) methods [127–130], with the glass frit used as a starting material. The additive manufacturing techniques usually require a high free flowing capability of the printed mixture. Spherical particles (glass microspheres) exhibit a much better free-flowing capability than anisotropic or platelet-like particles. The use of novel materials with specific physical properties, such as glass microspheres instead of conventional glass frits provides an additional advantage to the process by enhancing the flow and reducing the internal friction (viscosity) of printed formulations [131]. As a result, the influence on the rheology of the glass microspheres (viscosity, melt-flow, sintering, packing density etc.) is significantly lower in comparison to other, non-spherical, mineral fillers. Fig. 11a shows preliminary results of porous 3D glass scaffold preparation from SGMs in the borosilicate glass system. Fig. 11b shows the partially sintered glass microspheres at

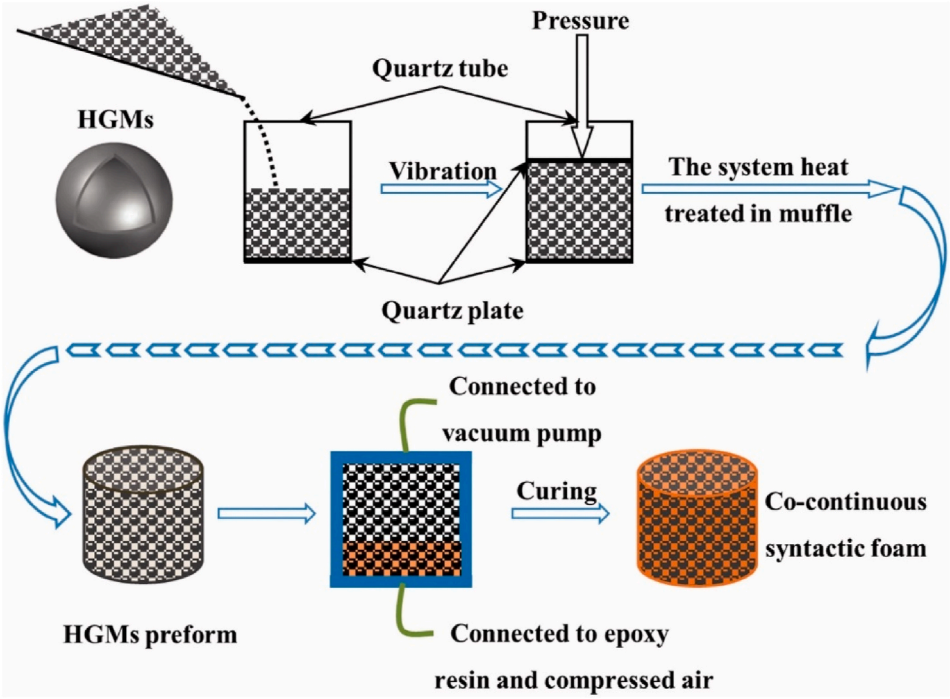

Fig. 10. Schematics of the co-continuous syntactic foam fabrication [114].

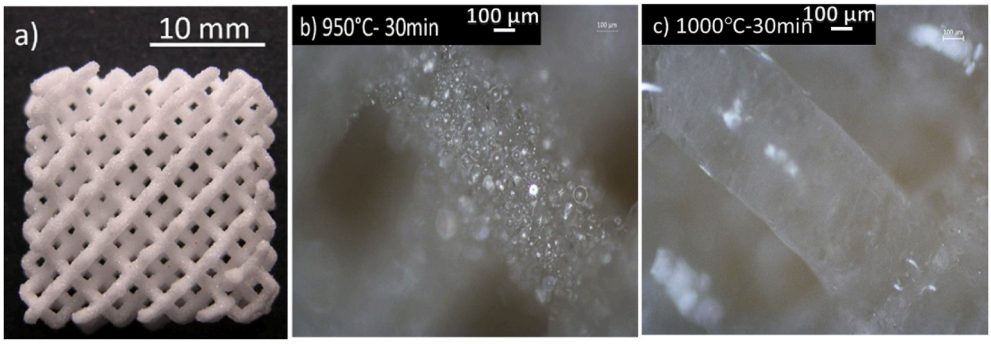

Fig. 11. Optical stereomicrograph of 3D glass scaffold after sintering at 950 °C for 30 min: a) Kelvin cell scaffold, b) open porosity of sintered glass microspheres at higher magnification, c) fused beam of glass microspheres sintered at 1000 °C for 30min at higher magnification.

950 °C. Increasing the sintering temperature to 1000 °C led to the formation of a fused beam of glass (Fig. 11c). The fabricated 3D scaffold shows potential for the use in optical applications.

Additive manufacturing technology can be also regarded as a new tool for upgrading waste glass. For instance, LCD glass waste is of interest due to its relatively high processing temperature and its resistance to crystallization. Fabrication of highly transparent scaffolds (based on LCD glass) suitable for the fabrication of innovative gas sensing devices is feasible by DIW [132]. The potential of masked SLA in the manufacture of more complex transparent components has been also identified [132]. Mahmoud et al. reused glass waste from discarded pharmaceutical vials for the fabrication of a new generation of monolithic sorbents for dye removal [133]. According to the study of Kraxner et al., by using glass microspheres instead of glass frit with irregular particles increased the maximum solid loading of the used glass waste in the ink from 55 wt % up to 77 wt% [134]. Masked SLA combined with a careful selection of sintering conditions enables the fabrication of components with tortuous porosity [133].

3D printing of glass microspheres represents the latest trend in additive manufacturing of glass. The future direction is to fabricate porous ceramic components of arbitrarily complex shapes for a wide range of applications including electronics, aerospace and biomedical engineering. Glass microspheres with tailored 3D structures can be employed for environmental remediation by adsorbing pollutants from water. Their high surface area and porosity enhance adsorption efficiency, contributing to cleaner water. Moreover, 3D-printed glass microspheres can be integrated into microfluidic devices, enabling precise control over fluid flow, mixing, and reactions. This can have applications in lab-on-a-chip systems for chemical analysis and diagnostics [135].

5.8.1. *Challenges for shaping glass microspheres by 3D printing*

Material compatibility, finding or developing glass materials suitable for 3D printing can be challenging. Glass has different thermal and mechanical properties compared to polymers commonly used in 3D printing, requiring specialized techniques and equipment. Printing resolution, achieving high-resolution 3D printing of glass microspheres can be technically demanding [134]. Precise control over print parameters, such as nozzle size and printing temperature for direct ink writing (DIW) and fused deposition modeling (FDM) techniques, is necessary to create intricate microsphere structures. Complex geometries, designing and printing complex 3D geometries in glass microspheres can be challenging, especially when aiming for specific shapes or internal

structures. Ensuring consistency and repeatability in production can be demanding. After 3D printing, glass microspheres may require additional post-processing steps, such as heat treatments, to enhance their mechanical and optical properties. These steps can add complexity to the manufacturing process [136].

6. Future of glass microspheres

The development of glass microspheres represents an exciting frontier in materials science and technology, holding immense potential for a wide array of applications. Looking towards the future, several profound discussions and perspectives can be identified to guide and accelerate the development of glass microspheres.

6.1. Tailored compositions and properties

Future research should focus on precisely tailoring the compositions of glass microspheres to achieve desired properties. Incorporating various materials or dopants into the glass matrix can enable enhanced functionalities such as controlled release of various substances, improved mechanical strength, and better thermal or electrical conductivity. Understanding the relationship between composition and properties will be crucial for developing microspheres that meet specific application requirements [41]. Sustainable manufacturing processes that facilitate environmentally sustainable synthesis of glass microspheres need to be a priority. Considering the environmental impact of manufacturing, efforts should be directed towards energy-efficient production methods, utilization of eco-friendly raw materials, and waste reduction during synthesis. Additionally, the incorporation of waste materials or by-products into the glass composition can be explored to promote sustainability [41].

6.2. Nanostructured glass microspheres

Integrating nanostructured features into glass microspheres can lead to innovative applications. Nanoscale modifications can influence surface reactivity, catalytic activity, and optical properties. The controlled synthesis of nanostructured glass microspheres may unlock new opportunities in catalysis, drug delivery, and nanotechnology, where precise control at the nanoscale is critical [73].

6.3. Functionalized surfaces and coatings

Surface modification and functionalization of glass microspheres present an exciting avenue for future development. By engineering surface coatings, microspheres can be designed to exhibit tailored interactions with specific substances or biological entities. This opens up opportunities in targeted drug delivery, enhanced adhesion in coatings, and effective pollutant adsorption [122].

6.4. Integration into advanced materials

Incorporating glass microspheres into advanced composite materials, such as high-performance polymers, ceramics, or concrete, can enhance properties and performance. By strategically designing composites with microspheres, it is possible to achieve lightweight, strong, and thermally efficient materials for aerospace, automotive, and construction applications [137]. Additive manufacturing, leveraging 3D printing for creating intricate structures using glass microspheres as building blocks holds immense potential. Custom-designed microsphere architectures could enable rapid prototyping of complex structures, customized implants, and advanced optical devices, paving the way for innovative applications in various sectors [138]. This applies also for multifunctional glass microspheres. Future research should aim at designing glass microspheres with multifunctional capabilities. Combining properties like magnetism, luminescence, and drug encapsulation within a single microsphere could lead to multifaceted applications, spanning from targeted drug delivery to magnetic resonance imaging contrast agents.

7. Conclusion

Environmental applications of glass microspheres have increased steadily over the past decades, paralleling advances in high-quality, large-batch production. Glass microspheres can be successfully prepared by flame synthesis, liquid droplet method, dry gel method or electrical arc method. The coating of glass microspheres by titania gives them a potential for photodegradation of the organic dye from wastewater. Due to their high specific surface area, PGMs are promising candidates for water filtration. The low density and thermal conductivity of HGMs allow them to be a beneficial lightweight filler in thermal insulating and road improvement materials. HGMs and PGMs are not only applicable in cementitious materials but also in energy applications such as active additives in lead acid batteries and safe storage material for hydrogen gas. Glass microspheres are advantageous in additive manufacturing of glass, allowing high solid loading (77 wt%) in the ink, thus maximizing the contact between adjacent particles and preventing the collapse of printed structures. The future of glass microspheres lies in their ability to be tailored, functionalized, and integrated into advanced materials and technologies. Collaborative efforts, coupled with advancements in materials characterization and manufacturing technologies, will be instrumental in unlocking the full potential of glass microspheres and driving innovative solutions across diverse fields.

Declaration of competing interest

The authors declare that they have no known competing financial interests or personal relationships that could have appeared to influence the work reported in this paper.

Acknowledgements

This paper is a part of the dissemination activities of project “FunGlass” (Centre for Functional and Surface Functionalized Glass). This project has received funding from the European Union’s Horizon 2020 research and innovation program under grant agreement no. 739566. Publication was created also in the frame of project: Advancement and support of R&D for Centre for diagnostics and quality testing of materials in the domains of the RIS3 SK specialization, ITMS2014+:313011W442, based on the Operational Program Integrated Infrastructure and funded from the European Regional Development Fund. Enrico Bernardo acknowledges the additional funding from the University of Padova (Dept. Of Industrial Engineering), in the framework of the “SusPIRe” (Sustainable porous ceramics from inorganic residues, BIRD202134). The authors also gratefully acknowledge the financial support from the Slovak Grant Agency of Ministry of Education, Science, Research and Sport, VEGA No 1/0456/20.

References

[1] B. Karasu, et al., Glass Microspheres, El-Cezeri Fen ve Mühendislik Dergisi, 2019, https://doi.org/10.31202/ecjse.562013.
[2] C.-T. Kung, et al., Microfluidic synthesis control technology and its application in drug delivery, bioimaging, biosensing, environmental analysis and cell analysis, Chem. Eng. J. 399 (2020), 125748, https://doi.org/10.1016/j.cej.2020.125748.
[3] Z. Wang, et al., Preparation of lightweight glass microsphere/Al sandwich composites with high compressive properties, Mater. Lett. 308 (2022), 131220, https://doi.org/10.1016/j.matlet.2021.131220.
[4] B. Zdravkov, et al., Pore classification in the characterization of porous materials: a perspective, Open Chem. 5 (2) (2007) 385–395, https://doi.org/10.2478/s11532-007-0017-9.
[5] M. Nagrath, et al., Tantalum-containing meso-porous glass fibres for hemostatic applications, Mater. Today Commun. 27 (2021), 102260, https://doi.org/10.1016/j.mtcomm.2021.102260.

[6] M. Huang, et al., NMR studies of materials loaded into porous-wall hollow glass microspheres, Mater. Sci. Eng., C 116 (2020), 111177, https://doi.org/10.1016/j.msec.2020.111177.

[7] G.C. Righini, Glassy microspheres for energy applications, Micromachines 9 (8) (2018) 1–18, https://doi.org/10.3390/mi9080379.

[8] S.E. Amos, B. Yalcin, Hollow Glass Microspheres for Plastics, Elastomers, and Adhesives Compounds, Elsevier, 2015.

[9] M.J. Zainorizuan, et al., Potential of hollow glass microsphere as cement replacement for lightweight foam concrete on thermal insulation performance, MATEC Web of Conferences 103 (2017), 01014, https://doi.org/10.1051/matecconf/201710301014.

[10] L. Li, et al., A novel etching and reconstruction route to ultrathin porous TiO2 hollow spheres for enhanced photocatalytic hydrogen evolution, Int. J. Hydrogen Energy 41 (3) (2016) 1627–1634, https://doi.org/10.1016/j.ijhydene.2015.10.110.

[11] M. Ozkutlu, C. Dilek, G. Bayram, Effects of hollow glass microsphere density and surface modification on the mechanical and thermal properties of poly(methyl methacrylate) syntactic foams, Compos. Struct. 202 (2018) 545–550, https://doi.org/10.1016/j.compstruct.2018.02.088.

[12] B. Zheng, et al., Buoyancy materials of aluminium borosilicate glass for high temperature resistance, Mater. Res. Innovat. 19 (sup4) (2015) S50–S53, https://doi.org/10.1179/1432891715z.0000000001515.

[13] O. Sandin, J. Nordin, M. Jonsson, Reflective properties of hollow microspheres in cool roof coatings, J. Coating Technol. Res. 14 (4) (2017) 817–821, https://doi.org/10.1007/s11998-017-9973-y.

[14] l.K. Heung, et al., Encapsulation of Palladium in Porous Wall Hollow Glass Microspheres, Materials Innovations in an Emerging Hydrogen Economy, 2009.

[15] G. Wicks, Nanostructures and "nanonothingness" in unique glass microspheres, Int. J. Appl. Glass Sci. 4 (2) (2013) 100–104, https://doi.org/10.1111/ijag.12031.

[16] M. Koopman, et al., Titania-coated glass microballoons and cenospheres for environmental applications, J. Mater. Sci. 44 (6) (2009) 1435–1441, https://doi.org/10.1007/s10853-008-2963-9.

[17] S.A. Krishna, et al., Biomedical applications of microspheres, Journal of Modern Drug Discovery and Drug Delivery Research (2015) 1–5.

[18] K.M.Z. Hossain, et al., Porous calcium phosphate glass microspheres for orthobiologic applications, Acta Biomater. 72 (2018) 396–406, https://doi.org/10.1016/j.actbio.2018.03.040.

[19] J. Kraxner, et al., Úžitkový vzor/Utility Model: Zariadenie Na Výrobu Plných, Dutých Alebo Pórovitých Sklených Alebo Sklo-Keramických Mikroguľôčok Pomocou Plameňovej Syntézy/Flame Synthesis Device for the Production of Solid, Hollow and Porous Glass and Glass-Ceramics Microspheres, 2020. číslo No. 8673.

[20] S.E. Amos, B. Yalçın, Hollow glass microspheres for plastics, elastomers, and adhesives compounds, in: PDL Handbook Series, William Andrew, Elsevier, 2015.

[21] A. Agrawal, S. Chandraker, A. Sharma, Physical, mechanical and sliding wear behavior of solid glass microsphere filled epoxy composites, Mater. Today: Proc. 29 (2020) 420–426, https://doi.org/10.1016/j.matpr.2020.07.295.

[22] H. Geng, et al., Fabrication of heat-resistant syntactic foams through binding hollow glass microspheres with phosphate adhesive, Mater. Des. 95 (2016) 32–38, https://doi.org/10.1016/j.matdes.2016.01.108.

[23] N. Gupta, et al., Characterization of mechanical and electrical properties of epoxy-glass microballoon syntactic composites, Ferroelectrics 345 (1) (2006) 1–12, https://doi.org/10.1080/00150190601018002.

[24] F. Schüth, Poröse Materialien im Überblick, Chem. Ing. Tech. 82 (6) (2010) 769–777, https://doi.org/10.1002/cite.201000063.

[25] B. Wu, et al., Epoxy-matrix composite with low dielectric constant and high thermal conductivity fabricated by HGMs/Al2O3 co-continuous skeleton, J. Alloys Compd. 869 (2021), 159332, https://doi.org/10.1016/j.jallcom.2021.159332.

[26] J.R. Martinelli, et al., Synthesis and characterization of glass–ceramic microspheres for thermotherapy, J. Non-Cryst. Solids 356 (44–49) (2010) 2683–2688, https://doi.org/10.1016/j.jnoncrysol.2010.05.006.

[27] N.R. Scott, et al., Experimental and computational characterization of glass microsphere-cementitious composites, Cement Concr. Res. 152 (2022), 106671, https://doi.org/10.1016/j.cemconres.2021.106671.

[28] A. Rosenflanz, et al., Bulk glasses and ultrahard nanoceramics based on alumina and rare-earth oxides, Nature 430 (7001) (2004) 761–764, https://doi.org/10.1038/nature02729.

[29] G. Zhao, et al., Flame synthesis of carbon nanotubes on glass fibre fabrics and their enhancement in electrical and thermal properties of glass fibre/epoxy composites, Compos. B Eng. 198 (2020), 108249, https://doi.org/10.1016/j.compositesb.2020.108249.

[30] N.J. Lakhkar, et al., Titanium phosphate glass microspheres for bone tissue engineering, Acta Biomater. 8 (11) (2012) 4181–4190, https://doi.org/10.1016/j.actbio.2012.07.023.

[31] J. Kraxner, et al., Porous bioactive glass microspheres prepared by flame synthesis process, Mater. Lett. 256 (2019), 126625, https://doi.org/10.1016/j.matlet.2019.126625.

[32] C.D. Hendricks, et al., Fabrication of glass sphere laser fusion targets, J. Nucl. Mater. 85–86 (1979) 107–111, https://doi.org/10.1016/0022-3115(79)90476-8.

[33] S.X. Qi Lin, X.D. Chen, Improving the glass-filament method for accurate measurement of drying kinetics of liquid droplets, Chem. Eng. Res. Des. 80 (4) (2002) 401–410, https://doi.org/10.1205/026387602317446443.

[34] K.J. Buschow, E.P.W, V. Christoph, Ferromagnetic Materials. A Handbook on the Properties of Magnetically Ordered Substances, 1991, https://doi.org/10.1002/crat.2170260703.

[35] Y. Lin, et al., Sol-gel MgO coating on glass microspheres for inhibiting excessive interfacial reaction in Al-Mg matrix syntactic foam, J. Alloys Compd. 798 (2019) 59–66, https://doi.org/10.1016/j.jallcom.2019.05.258.

[36] R.D. Hunt, J.L. Collins, J.S. Choi, Key properties of mixed cerium and zirconium microspheres prepared by the internal gelation process with previously boiled HMTA and urea, Ceram. Int. 47 (16) (2021) 23295–23299, https://doi.org/10.1016/j.ceramint.2021.05.042.

[37] S. Wang, W.J, C. Wang, Z. Ma, W. Man, Synthesis of carbon nanotubes by MWPCVD at low temperature, Plasma Sci. Technol. 4 (2002) 1135–1140.

[38] K. S.O, Principles of Electrical Engineering Materials and Devices, McGraw Hill, Boston, MA, 1997.

[39] I. Bica, Formation of glass microspheres with rotating electrical arc, Mater. Sci. Eng., B 77 (2) (2000) 210–212, https://doi.org/10.1016/s0921-5107(00)00483-9.

[40] J.-L. Hu, et al., Silica-based hybrid microspheres: synthesis, characterization and wastewater treatment, RSC Adv. 3 (48) (2013), 25620, https://doi.org/10.1039/c3ra44111c.

[41] M. Mahmoud, et al., Porous glass microspheres from alkali-activated fiber glass waste, Materials 15 (3) (2022) 1043, https://doi.org/10.3390/ma15031043.

[42] A. Vignali, et al., Lightweight poly(epsilon-caprolactone) composites with surface modified hollow glass microspheres for use in rotational molding: thermal, rheological and mechanical properties, Polymers 11 (4) (2019), https://doi.org/10.3390/polym11040624.

[43] A. Belostozky, et al., Solidification of oil liquids by encapsulation within porous hollow silica microspheres of narrow size distribution for pharmaceutical and cosmetic applications, Mater. Sci. Eng., C 97 (2019) 760–767, https://doi.org/10.1016/j.msec.2018.12.093.

[44] S.A. Samad, et al., Upcycling glass waste into porous microspheres for wastewater treatment applications: efficacy of dye removal, Materials 15 (17) (2022), https://doi.org/10.3390/ma15175809.

[45] F. Aslani, L. Wang, Development of strain-hardening lightweight engineered cementitious composites using hollow glass microspheres, Struct. Concr. 21 (2) (2019) 673–688, https://doi.org/10.1002/suco.201900096.

[46] C. Feng, et al., The effects of hollow glass microsphere modification on the road performances and thermal performance of asphalt binder and mixture, Construct. Build. Mater. 220 (2019) 64–75, https://doi.org/10.1016/j.conbuildmat.2019.05.183.

[47] S. Dalai, V. Savithri, P. Sharma, Investigating the effect of cobalt loading on thermal conductivity and hydrogen storage capacity of hollow glass microspheres (HGMs), Mater. Today: Proc. 4 (11) (2017) 11608–11616, https://doi.org/10.1016/j.matpr.2017.09.072.

[48] G.C. Righini, Glassy microspheres for energy applications, Micromachines 9 (8) (2018), https://doi.org/10.3390/mi9080379.

[49] M. Michálková, et al., Viscous flow spark plasma sintering of glass microspheres with YAG composition and high tendency to crystallization, J. Eur. Ceram. Soc. 41 (2) (2021) 1537–1542, https://doi.org/10.1016/j.jeurceramsoc.2020.10.015.

[50] H.S. Ningsih, et al., Effects of strontium dopants on the in vitro bioactivity and cytotoxicity of strontium-doped spray-dried bioactive glass microspheres, J. Non-Cryst. Solids 576 (2022), 121284, https://doi.org/10.1016/j.jnoncrysol.2021.121284.

[51] P. Wang, et al., Measurement and calculation of cryogenic thermal conductivity of HGMs, Int. J. Heat Mass Tran. 129 (2019) 591–598, https://doi.org/10.1016/j.ijheatmasstransfer.2018.09.113.

[52] V.V. Budov, Hollow glass microspheres. use, properties, and technology (Review), Glass Ceram. 51 (7) (1994) 230–235, https://doi.org/10.1007/BF00680655.

[53] S. Dalai, et al., Preparation and characterization of hollow glass microspheres (HGMs) for hydrogen storage using urea as a blowing agent, Microelectron. Eng. 126 (2014) 65–70, https://doi.org/10.1016/j.mee.2014.06.017.

[54] D. Kang, et al., Effect of hollow glass microsphere (HGM) on the dispersion state of single-walled carbon nanotube (SWNT), Compos. B Eng. 117 (2017) 35–42, https://doi.org/10.1016/j.compositesb.2017.02.038.

[55] B. Zhu, et al., Thermal, dielectric and compressive properties of hollow glass microsphere filled epoxy-matrix composites, J. Reinforc. Plast. Compos. 31 (19) (2012) 1311–1326, https://doi.org/10.1177/0731684412452918.

[56] J. Kraxner, et al., Production of Hollow Glass Microspheres with Na2SO4 Blowing Agent in Processing and Properties of Advanced Ceramics and Glass Conference, 2017, pp. 56–61.

[57] J.-Z. Liang, Macromol. Mater. Eng. 287 (9) (2002) 588–591, https://doi.org/10.1002/1439-2054(20020901)287:9<588::aid-mame588>3.0.co;2-6.

[58] M.T. Islam, et al., Rapid conversion of highly porous borate glass microspheres into hydroxyapatite, Biomater. Sci. 9 (5) (2021) 1826–1844, https://doi.org/10.1039/d0bm01776k.

[59] S.A. Samad, et al., Adsorption studies and effect of heat treatment on porous glass microspheres, Int. J. Appl. Glass Sci. (2021), https://doi.org/10.1111/ijag.16352.

[60] F. Pacheco-Torgal, J. Castro-Gomes, S. Jalali, Alkali-activated binders: a review, Construct. Build. Mater. 22 (7) (2008) 1305–1314, https://doi.org/10.1016/j.conbuildmat.2007.10.015.

[61] C.E. White, et al., Intrinsic differences in atomic ordering of calcium (alumino) silicate hydrates in conventional and alkali-activated cements, Cement Concr. Res. 67 (2015) 66–73, https://doi.org/10.1016/j.cemconres.2014.08.006.

[62] C. Li, H. Sun, L. Li, A review: the comparison between alkali-activated slag (Si+Ca) and metakaolin (Si+Al) cements, Cement Concr. Res. 40 (9) (2010) 1341–1349, https://doi.org/10.1016/j.cemconres.2010.03.020.

[63] C.K. Yip, et al., Effect of calcium silicate sources on geopolymerisation, Cement Concr. Res. 38 (4) (2008) 554–564, https://doi.org/10.1016/j.cemconres.2007.11.001.
[64] Y. Yang, et al., Shallow porous microsphere carriers with core-shell structure based on glass beads cross-linking chitosan for immobilizing inulinase, Mol. Catal. 486 (2020), 110871, https://doi.org/10.1016/j.mcat.2020.110871.
[65] W. Hong, et al., A hierarchically porous bioactive glass-ceramic microsphere with enhanced bioactivity for bone tissue engineering, Ceram. Int. 45 (10) (2019) 13579–13583, https://doi.org/10.1016/j.ceramint.2019.03.241.
[66] G.R. Guillen, et al., Preparation and characterization of membranes formed by nonsolvent induced phase separation: a review, Ind. Eng. Chem. Res. 50 (7) (2011) 3798–3817, https://doi.org/10.1021/ie101928r.
[67] G.G. Wicks, et al., Microspheres and Microworlds, vol. 87, American Ceramic Society Bulletin, 2008, pp. 23–28.
[68] M.T. Islam, et al., Effect of varying the Mg with Ca content in highly porous phosphate-based glass microspheres, Mater. Sci. Eng., C 120 (2021), 111668, https://doi.org/10.1016/j.msec.2020.111668.
[69] M. Kukizaki, Large-scale production of alkali-resistant Shirasu porous glass (SPG) membranes: influence of ZrO2 addition on crystallization and phase separation in Na2O–CaO–Al2O3–B2O3–SiO2 glasses; and alkali durability and pore morphology of the membranes, J. Membr. Sci. 360 (1–2) (2010) 426–435, https://doi.org/10.1016/j.memsci.2010.05.042.
[70] M. Hasanuzzaman, A.R.M. Harunur Rashid, A.-G. Olabi, Characterization of porous glass and ceramics by mercury intrusion porosimetry, in: Book: Reference Module in Materials Science and Materials Engineering, 2017, https://doi.org/10.1016/b978-0-12-803581-8.09266-3.
[71] W. Skatulla, et al., Phase separation and boron anomaly in simple sodium borate and technical alkali-borosilicate glasses, Silikat Technol 9 (1958) 51–62.
[72] T.E. Sadrabadi, et al., Characterization of micro/nano porous hollow glass microspheres fabricated through various chemical etching process for use in smart coatings Iranian, J. Mater. Sci. Eng. 13 (4) (2016) 1–9.
[73] S. Li, et al., Porous-wall hollow glass microspheres as novel potential nanocarriers for biomedical applications, Nanomedicine 6 (1) (2010) 127–136, https://doi.org/10.1016/j.nano.2009.06.004.
[74] S.S. Moosavi, P. Alizadeh, Effect of acid leaching time on pore diameter and volume of porous hollow glass microspheres, Mater. Lett. 167 (2016) 98–101, https://doi.org/10.1016/j.matlet.2015.12.114.
[75] K. Li, et al., Hermetically sealed porous-wall hollow microspheres enabled by monolithic glass coatings: potential for thermal insulation applications, Vacuum 195 (2022), 110667, https://doi.org/10.1016/j.vacuum.2021.110667.
[76] N.J. Lakhkar, Phosphate Glass Microspheres as Cell Microcarrier Substrates for Bone Tissue Engineering Applications, University College London, 2014.
[77] Q. Wang, et al., Preparation of hollow hydroxyapatite microspheres, J. Mater. Sci. Mater. Med. 17 (7) (2006) 641–646, https://doi.org/10.1007/s10856-006-9227-5.
[78] A. Matamoros-Veloza, et al., Formulating injectable pastes of porous calcium phosphate glass microspheres for bone regeneration applications, J. Mech. Behav. Biomed. Mater. 102 (2020), 103489, https://doi.org/10.1016/j.jmbbm.2019.103489.
[79] A. Konbul, E.M. Ozbayoglu, C. Mata, Survival of hollow glass microspheres in drilling fluids applications – effect of drill bit/formation contact, J. Petrol. Sci. Eng. 189 (2020), 106966, https://doi.org/10.1016/j.petrol.2020.106966.
[80] K.J. Krakowiak, et al., Engineering of high specific strength and low thermal conductivity cementitious composites with hollow glass microspheres for high-temperature high-pressure applications, Cement Concr. Compos. 108 (2020), 103514, https://doi.org/10.1016/j.cemconcomp.2020.103514.
[81] R. Xu, W. Wang, D. Yu, Preparation of silver-plated Hollow Glass Microspheres and its application in infrared stealth coating fabrics, Prog. Org. Coating 131 (2019) 1–10, https://doi.org/10.1016/j.porgcoat.2019.02.009.
[82] B. Sayinli, et al., Recent progress and challenges facing ballast water treatment - a review, Chemosphere (2021), 132776, https://doi.org/10.1016/j.chemosphere.2021.132776.
[83] C.-Y. Chen, W.J. Tseng, Preparation of TiN-WN composite particles for selective adsorption of methylene blue dyes in water, Adv. Powder Technol. (2022), 103423, https://doi.org/10.1016/j.apt.2021.103423.
[84] G. Singh, M. Sharma, R. Vaish, Emerging trends in glass-ceramic photocatalysts, Chem. Eng. J. 407 (2021), 126971, https://doi.org/10.1016/j.cej.2020.126971.
[85] A. El Yadini, et al., Supported TiO2 on borosilicate glass plates for efficient photocatalytic degradation of fenamiphos, Journal of Catalysts 2014 (2014) 1–8, https://doi.org/10.1155/2014/413693.
[86] J.S. Park, et al., Hetero-structured palladium-coated zinc oxide photocatalysts for sustainable water treatment, J. Water Proc. Eng. 45 (2022), 102488, https://doi.org/10.1016/j.jwpe.2021.102488.
[87] A. Fujishima, X. Zhang, D. Tryk, TiO2 photocatalysis and related surface phenomena, Surf. Sci. Rep. 63 (12) (2008) 515–582, https://doi.org/10.1016/j.surfrep.2008.10.001.
[88] X. Zhang, Cr/S/TiO2-loaded Hollow Glass Microspheres as an Efficient and Recyclable Catalyst for the Photocatalytic Degradation of Indigo Carmine under Visible Light, Química Nova, 2016, https://doi.org/10.21577/0100-4042.20160121.
[89] Y. An, et al., Functioned hollow glass microsphere as a self-floating adsorbent: rapid and high-efficient removal of anionic dye, Hazard Material 381 (2020), 120971, https://doi.org/10.1016/j.jhazmat.2019.120971.
[90] S.G. Gunnarsson, Self Cleaning Paint: Introduction of Photocatalytic Particles into a Paint System, Technical University of Denmark, 2012.
[91] B. Li, et al., Effect of microstructure and physical parameters of hollow glass microsphere on insulation performance, Mater. Lett. 65 (12) (2011) 1992–1994, https://doi.org/10.1016/j.matlet.2011.03.062.
[92] R.E. Skochdopole, The thermal conductivity of foamed plastics, Chem. Eng. Prog. 88 (1961) 55–57.
[93] J. Long, et al., Controlled TiO2 coating on hollow glass microspheres and their reflective thermal insulation properties, Particuology 49 (2020) 33–39, https://doi.org/10.1016/j.partic.2019.03.002.
[94] Y. Hu, et al., Silicon rubber/hollow glass microsphere composites: influence of broken hollow glass microsphere on mechanical and thermal insulation property, Compos. Sci. Technol. 79 (2013) 64–69, https://doi.org/10.1016/j.compscitech.2013.02.015.
[95] J. Xu, et al., Effects of hollow glass beadson light-reflecting and heat-insulating properties of coating, Mater. Sci. Eng. 30 (2012) 347–351.
[96] D. Oreshkin, V. Semenov, T. Rozovskaya, Properties of light-weight extruded concrete with hollow glass microspheres, Procedia Eng. 153 (2016) 638–643, https://doi.org/10.1016/j.proeng.2016.08.214.
[97] N. Kumar, et al., Light-weight high-strength hollow glass microspheres and bamboo fiber based hybrid polypropylene composite: a strength analysis and morphological study, Compos. B Eng. 109 (2017) 277–285, https://doi.org/10.1016/j.compositesb.2016.10.052.
[98] K. Yan, et al., Storage of hydrogen by high pressure microencapsulation in glass, Int. J. Hydrogen Energy 10 (7–8) (1985) 517–522, https://doi.org/10.1016/0360-3199(85)90081-3.
[99] J.E. Shelby, et al., Fuels-hydrogen Storage: Hydrogen Storage in Glass Microspheres, Encyclopedia of electrochemical power sources, 2009, pp. 488–492.
[100] D. Kohli, et al., Glass micro-container based hydrogen storage scheme, Int. J. Hydrogen Energy 33 (1) (2008) 417–422, https://doi.org/10.1016/j.ijhydene.2007.07.044.
[101] J.E. Shelby, F.C. Raszewski, M.M. Hall, FUELS – HYDROGEN STORAGE, Glass Microspheres, 2009, pp. 488–492, https://doi.org/10.1016/b978-044452745-5.00334-8.
[102] M. Nogami, et al., Fabrication of hollow glass microspheres in the Na2O-B2O3-SiO2 system from metal alkoxides, Mater. Sci. Eng. 17 (1982) 2845–2890.
[103] M.L. Schmitt, J.E. Shelby, M.M. Hall, Preparation of hollow glass microspheres from sol–gel derived glass for application in hydrogen gas storage, J. Non-Cryst. Solids 352 (6–7) (2006) 626–631, https://doi.org/10.1016/j.jnoncrysol.2005.11.057.
[104] S. Shetty, M. Hall, Facile production of optically active hollow glass microspheres for photo-induced outgassing of stored hydrogen, Int. J. Hydrogen Energy 36 (16) (2011) 9694–9701, https://doi.org/10.1016/j.ijhydene.2011.04.195.
[105] J.H. Campbell, et al., Preparation and Properties of Hollow Glass Microspheres for Use in Laser Fusion Experiments, United States: N. P., 1983 https://doi.org/10.2172/6185129.
[106] X. Qi, et al., Production and characterization of hollow glass microspheres with high diffusivity for hydrogen storage, Int. J. Hydrogen Energy 37 (2) (2012) 1518–1530, https://doi.org/10.1016/j.ijhydene.2011.10.034.
[107] M.N. Channell, et al., Toward 3D printed hydrogen storage materials made with ABS-MOF composites, Polym. Adv. Technol. 29 (2) (2018) 867–873, https://doi.org/10.1002/pat.4197.
[108] S. Dalai, et al., Magnesium and iron loaded hollow glass microspheres (HGMs) for hydrogen storage, Int. J. Hydrogen Energy 39 (29) (2014) 16451–16458, https://doi.org/10.1016/j.ijhydene.2014.03.062.
[109] H. Behret, H. Binder, Lead-acid batteries, Ber. Bunsen Ges. Phys. Chem. 82 (6) (1978) 665–666, https://doi.org/10.1002/bbpc.197800141.
[110] D. Berndt, Maintenance-Free Batteries, John Wiley & Sons, New York, 1997.
[111] A.V.O. Akowanou, et al., 3D-printed clay-based ceramic water filters for point-of-use water treatment applications, Progress in Additive Manufacturing 4 (3) (2019) 315–321, https://doi.org/10.1007/s40964-019-00091-9.
[112] M. Sorge, et al., Investigating the use of porous, hollow glass microspheres in positive lead acid battery plates, J. Power Sources 266 (2014) 496–511, https://doi.org/10.1016/j.jpowsour.2014.05.021.
[113] B. Yalcin, S.E. Amos, Hollow Glass Microspheres in Thermoplastics, 2015, pp. 35–105, https://doi.org/10.1016/b978-1-4557-7443-2.00003-7.
[114] J. Ding, et al., Co-continuous hollow glass microspheres/epoxy resin syntactic foam prepared by vacuum resin transfer molding, J. Reinforc. Plast. Compos. 38 (19–20) (2019) 896–909, https://doi.org/10.1177/0731684419857173.
[115] 3M Case Study “Glass Bubbles Reduce Weight of TPO Parts” 3M Website.
[116] A.n. Salazar, On thermal diffusivity, Eur. J. Phys. 24 (4) (2003) 351–358, https://doi.org/10.1088/0143-0807/24/4/353.
[117] G. Yang, A.D. Migone, K.W. Johnson, Heat capacity and thermal diffusivity of a glass sample, Phys. Rev. B Condens. Matter 45 (1) (1992) 157–160, https://doi.org/10.1103/physrevb.45.157.
[118] G. Wang, R. Roque, D. Morian, Effects of surface rutting on near-surface pavement responses based on a two-dimensional axle-tire-pavement interaction finite-element model, J. Mater. Civ. Eng. 24 (11) (2012) 1388–1395, https://doi.org/10.1061/(asce)mt.1943-5533.0000526.
[119] D. Yinfei, S. Qin, W. Shengyue, Highly oriented heat-induced structure of asphalt pavement for reducing pavement temperature, Energy Build. 85 (2014) 23–31, https://doi.org/10.1016/j.enbuild.2014.09.035.
[120] A. Sha, et al., Solar heating reflective coating layer (SHRCL) to cool the asphalt pavement surface, Construct. Build. Mater. 139 (2017) 355–364, https://doi.org/10.1016/j.conbuildmat.2017.02.087.

[121] Y. Du, et al., Evaluation of thermal and anti-rutting behaviors of thermal resistance asphalt pavement with glass microsphere, Construct. Build. Mater. 263 (2020), 120609, https://doi.org/10.1016/j.conbuildmat.2020.120609.
[122] D.-Y. Shin, K. Kimura, Preparation of TiO2-coated hollow glass microspheres from titania-hydrate-coated fine volcanic glass, J. Ceram. Soc. Jpn. 107 (1249) (1999) 775–779, https://doi.org/10.2109/jcersj.107.775.
[123] C. Liu, et al., Additive manufacturing of silica glass using laser stereolithography with a top-down approach and fast debinding, RSC Adv. 8 (29) (2018) 16344–16348, https://doi.org/10.1039/c8ra02428f.
[124] I. Cooperstein, et al., Additive manufacturing of transparent silica glass from solutions, ACS Appl. Mater. Interfaces 10 (22) (2018) 18879–18885, https://doi.org/10.1021/acsami.8b03766.
[125] F. Kotz, et al., Three-dimensional printing of transparent fused silica glass, Nature 544 (7650) (2017) 337–339, https://doi.org/10.1038/nature22061.
[126] J. Klein, et al., Additive manufacturing of optically transparent glass, 3D Print. Addit. Manuf. 2 (3) (2015) 92–105, https://doi.org/10.1089/3dp.2015.0021.
[127] J. Schmidt, et al., Digital light processing of wollastonite-diopside glass-ceramic complex structures, J. Eur. Ceram. Soc. 38 (13) (2018) 4580–4584, https://doi.org/10.1016/j.jeurceramsoc.2018.06.004.
[128] G. Franchin, et al., Removal of ammonium from wastewater with geopolymer sorbents fabricated via additive manufacturing, Mater. Des. 195 (2020), 109006, https://doi.org/10.1016/j.matdes.2020.109006.
[129] H. Elsayed, P. Colombo, E. Bernardo, Direct ink writing of wollastonite-diopside glass-ceramic scaffolds from a silicone resin and engineered fillers, J. Eur. Ceram. Soc. 37 (13) (2017) 4187–4195, https://doi.org/10.1016/j.jeurceramsoc.2017.05.021.
[130] J. Bauer, C. Crook, T. Baldacchini, A sinterless, low-temperature route to 3D print nanoscale optical-grade glass, Science 380 (6648) (2023) 960–966, https://doi.org/10.1126/science.abq3037.
[131] Malvern Instruments, Optimizing Metal Powders for Additive Manufacturing - Exploring the Impact of Particle Morphology and Powder Flowability, 2017. https://www.malvernpanalytical.com/.
[132] A. Dasan, et al., Up-cycling of LCD glass by additive manufacturing of porous translucent glass scaffolds, Materials 14 (17) (2021), https://doi.org/10.3390/ma14175083.
[133] M. Mahmoud, et al., Advanced dye sorbents from combined stereolithography 3D printing and alkali activation of pharmaceutical glass waste, Materials 15 (2022) 6823, https://doi.org/10.3390/ma15196823.
[134] J. Kraxner, et al., Additive manufacturing of Ca–Mg silicate scaffolds supported by flame-synthesized glass microspheres, Ceram. Int. (2021), https://doi.org/10.1016/j.ceramint.2021.12.095.
[135] S. Arshavsky-Graham, et al., 3D-printed microfluidics integrated with optical nanostructured porous aptasensors for protein detection, Mikrochim. Acta 188 (3) (2021) 67, https://doi.org/10.1007/s00604-021-04725-0.
[136] A. Dasan, et al., 3D printing of hierarchically porous lattice structures based on akermanite glass microspheres and reactive silicone binder, J. Funct. Biomater. 13 (1) (2022), https://doi.org/10.3390/jfb13010008.
[137] L.C. Herrera-Ramírez, M. Cano, R. Guzman de Villoria, Low thermal and high electrical conductivity in hollow glass microspheres covered with carbon nanofiber–polymer composites, Compos. Sci. Technol. 151 (2017) 211–218, https://doi.org/10.1016/j.compscitech.2017.08.020.
[138] J. Kraxner, et al., Additive manufacturing of Ca–Mg silicate scaffolds supported by flame-synthesized glass microspheres, Ceram. Int. 48 (7) (2022) 9107–9113, https://doi.org/10.1016/j.ceramint.2021.12.095.